Journal of King Saud University – Computer and Information Sciences 31 (2019) 208–217

Contents lists available at ScienceDirect

Journal of King Saud University – Computer and Information Sciences

journal homepage: www.sciencedirect.com

A wavelet based approach for simultaneous compression and encryption of fused images

Ankita Vaish *, Sonam Gautam, Manoj Kumar

Department of Computer Science, Babasaheb Bhimrao Ambedkar University (A Central University), Lucknow 226025, India

ARTICLE INFO

Article history:
Received 4 November 2016
Accepted 24 January 2017
Available online 11 February 2017

Keywords:
Image compression
Image fusion
Image encryption
Pseudo random number sequence
Wavelet transform

ABSTRACT

This paper presents, a wavelet based technique to compress and secure the fused images in a dependent way. The core idea behind the proposed work lies in the selection of significant and less significant information in the wavelet domain. The significant wavelet coefficients are fused using error measurements while the less significant coefficients are fused by using maximum method, the fused information of significant wavelet coefficients is compressed and encrypted using error measurement and pseudo random number sequences, while the less significant fused coefficients are compressed using a quantizing parameter, the quantized values are pseudo randomly permuted and coded using huffman coding. At receiver side, the fused image can be recovered by using the proposed recovery algorithm. Numerical and visible results demonstrate the superiority of our technique over several other techniques.

1. Introduction

In the ever growing field of digital technologies, image fusion, encryption and compression are very hot topics of image processing and computer vision. Fusion is the process of integrating multisource images into a single visually improved image which can better describe the scene. Encryption is used for secure transmission of information, while compression is used to reduce the total number of bits required for image data which helps in fast transmission with reduced storage cost.

Image fusion can be defined as a process of integrating significant information of multiple source images of the same scene into a single visually improved image. The obtained image describes the whole information of the scene which is useful for human perception and image processing tasks. Image fusion has been employed in various fields, such as medical imaging, surveillance, robotics, machine vision, remote sensing and so on (Wald, 1999). The main objective of image fusion is to make a fused image more informative and better visual quality without presenting any artifacts. Usually, images of same scene having different focuses do not provide an image with every object in focus. To obtain an image with all scene in focus a multifocus image fusion approach has been introduced. If the images are taken from different sensors, the information obtained from different sensors is limited. These details of different sensor images are integrated to obtain the information of all images into a single enhanced image containing information obtained from both the sensors. The process of combining the details of different sensors images into a single image is known as the multisensor image fusion. Image fusion can be divided into pixel, feature and decision levels, where decision level is the highest level and pixel level is the lowest level (Blum and Liu, 2005). Pixel level fusion, basically perform pixel by pixel fusion. It is time efficient and simple to use, therefore it is most suitable for image fusion purpose. Image fusion techniques can be categorized into two groups: spatial and transform domains. The spatial domain methods are easy to implement but it may provide low contrast and insufficient details. To overcome these problems, transform domain based approaches have been introduced. Transform domain methods usually transform the images into multi-scale representation and then choose the decomposed details to obtain the fused image. There are some example of transform domain based fusion methods such as, discrete wavelet transform (DWT) (Li et al., 1995; Pajares and Cruz, 2004), contourlet transform (Liu et al., 2011), curvelet transform (Choi et al., 2005), dual tree complex wavelet transform (DT-CWT) (Kingsbury, 1999), and so on. A medical image fusion technique is given in Jigneshkumar and Mehul (2016), which can fuse the source images using DWT. Bhavana and Krishnappa (2016) proposed an image fusion technique for MRI and PET brain images using DWT and adaptive

* Corresponding author.
E-mail addresses: av21lko@gmail.com (A. Vaish), sonam870115@gmail.com (S. Gautam), mkjnuiitr@gmail.com (M. Kumar).
Peer review under responsibility of King Saud University.

Production and hosting by Elsevier

http://dx.doi.org/10.1016/j.jksuci.2017.01.005
1319-1578/

histogram equalization. By varying the structural information in the gray matter area and the spectral information in the white matter area, this technique (Bhavana and Krishnappa, 2016) provides satisfactory results.

Now a days, simultaneous image compression and encryption techniques are developed most frequently. A lot of image encryption and compression methods are reported in literature that are based on compressive sensing (CS) viz: an image encryption technique while reducing the storage space is given by Zhou et al. (2014), which gives good key distribution and saves large storage space. An image encryption technique using CS and classical double random phase encoding is proposed by Lu et al. (2013) which reduces the storage space while enhancing the security using Arnold transform (Liu et al., 2013). By combining CS and nonlinear fractional Mellin transform, an image encryption method is given in Zhou et al. (2015). A parallel image encryption technique is given by Huang et al. (2012) which is based on CS in this technique the block cipher structures consisting of scrambling, mixing, S-box and chaotic lattice XOR is developed to further encrypt the quantized data. A hybrid compression and encryption method with key-controlled measurement matrix in CS is proposed by Zhou et al. (2014). Further, a new CS based hybrid compression-encryption algorithm is given in Zhou et al. (2014), where measurement matrix is constructed as partial Hadamard matrix and controlled by a chaos index sequence. An image compression and encryption technique based on 2D CS and fractional Mellin transform (FrMT) is again proposed by Zhou et al. (2015) which uses the nonlinearity of FrMT to resist the common attacks and maintain the compression ability of CS. Alfalou and Brosseau (2009) proposed an optical image compression and encryption technique which is devoted for secure and efficient transmission of images over internet. For multiplexing and simultaneously encoding images, an other compression method is given in Alfalou et al. (2011). A simultaneous compression and encryption method is given by Zhou et al. (2016) using hyper-chaotic system and 2D CS, in this work CS is used to reduce the data size and then the compressed encrypted image is re-encrypted by using the cycle shift operation controlled by the hyper-chaotic system. A secure and efficient technique for simultaneous compression and encryption is given in Alfalou et al. (2010), where, compression and encryption of digital holograms for 3-D object reconstruction is implemented.

Generally, the above mentioned techniques are used in various application of image processing for a specific purpose. However, simultaneous implementation of these techniques has a wider application prospects. For an example, in case of tele-medicine, the multi-modal medical images need to be fused to incorporate the complementary information, meanwhile the security of transmitting information is necessary to maintain the privacy of patients. In military surveillance, visible and infrared images are fused to obtain an enhanced image with better visual quality and then fused information need to be encrypted for secure transmission over the network. In the aforementioned applications, it is indeed necessary to reduce the size of transmitting information while maintaining their security and entire visual information. Hence, it is really a great idea to study and implement image fusion, encryption and compression simultaneously in a proper way.

Recently, more attention has been paid on the study of simultaneous compression and encryption of fused images. viz: a simultaneous compression and encryption technique is given by Alfalou et al. (2013), this technique is a combination of spectral fusion based on the properties of Discrete Cosine Transformation (DCT). Zhu et al. (2013) proposed an efficient method using hyper-chaos and Chinese remainder theorem where 2-D hyper chaos is used to shuffle the original image and to diffuse and reduce the shuffled image simultaneously, Chinese remainder theorem is used. Apart from the above discussed methods, Multi-scale transform (MST) based methods are also useful in various applications of image processing. Few classical methods for image fusion are Laplacian pyramid (LP) (Burt and Adelson, 1983), ratio of low-pass pyramid (RP) (Toet, 1989), discrete wavelet transform (DWT) (Li et al., 1995), dual-tree complex wavelet transform (DTCWT) (Lewis et al., 2007) and curvelet transform (CVT) (Nencini et al., 2007). The intrinsic features of these transform based fusion methods gives us a new direction in the field of simultaneous fusion, encryption and compression (SFEC). Recently, simultaneous fusion, encryption and compression based methods are also developed more frequently viz: a discrete cosine transformation (DCT) based SFEC method is given by Alfalou et al. (2011), a SFEC technique is given in Alfalou et al. (2007), which can optimism the transmission of image while maintaining the security. A novel image fusion technique for visible and infrared images is given by Liu et al. (2014). More recently, a simultaneous compression, fusion and encryption technique is given by Liu et al. (2016) using CS and chaos.

In this article, a MST based simultaneous fusion, encryption and compression technique is proposed in wavelet domain. The multiresolution and energy compaction ability of wavelet has brought our attention to accomplish these tasks simultaneously. At first, the source images are wavelet transformed to form a sparse representation of data. The wavelet transform decomposes an image into an approximation and three detail wavelet sub-bands. The transformed coefficients in approximation sub-bands are not sparse and contain the most useful information of image therefore, termed as significant coefficients while the coefficients in the detail sub-bands are close to sparse and contain comparatively less information (termed as less significant coefficients). To fuse the coefficients of approximation subbands a scheme based on error measurements is used while for the fusion of high frequency coefficients containing low energy information maximum rule is used. The fused information of low and high frequency coefficients is encrypted and compressed simultaneously using the proposed encryption and compression technique.

The rest of the paper is organized as follows: a brief overview of Discrete wavelet transform (DWT) is given in Section 2, Section 3 describes the proposed simultaneously fusion, encryption and compression technique in detail, the experimental validation of proposed work with security analysis and compression performance is discussed in Section 4. Section 5 concludes the proposed work.

2. Discrete wavelet transform

Discrete Wavelet Transform (DWT) has been used more frequently in many applications of image processing like image compression, image encryption, fusion etc. DWT is localized both in time and frequency domains, which reveals the spatial and frequency views at the same time. It decomposes the image at multiresolution level, which helps in analyzing an image at different resolutions. Due to the multiresolution property of DWT, the information that seems to be unnoticed at one level may become noticeable at another level.

The 2-D DWT can be obtained by first applying 1-D DWT in horizontal direction and then in vertical direction. 2-D DWT decomposes an image into four parts: approximation (LL), horizontal (LH), vertical (HL) and diagonal (HH). LL subband contains low frequency detail, while the LH, HL and HH subbands contain the high frequency details (shown in Fig. 1).

For an image of size $M \times N$, 2-D DWT can be defined as (Gonzalez and Woods, 2013; Kumar and Vaish, 2016):

$$W_{\Phi}(j_0, m, n) = \frac{1}{MN}\sum_{x=0}^{M-1}\sum_{y=0}^{N-1} f(x,y)\Phi_{j_0,m,n}(x,y) \quad (1)$$

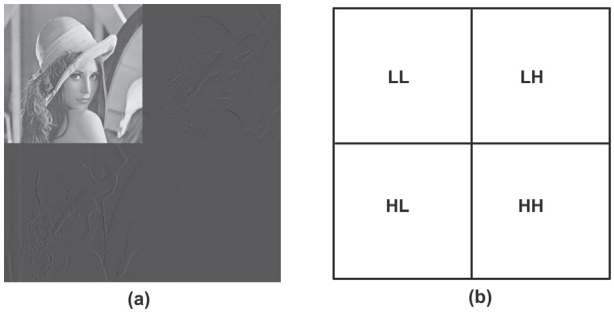

Fig. 1. One level wavelet decomposition.

$$W^i_{\Psi}(j,m,n)=\frac{1}{MN}\sum_{x=0}^{M-1}\sum_{y=0}^{N-1}f(x,y)\Psi^i_{j,m,n}(x,y) \tag{2}$$

where, $W_{\Phi}(j_0,m,n)$ represents approximation part and $W^i_{\Psi}(j,m,n)$ represents horizontal, vertical and diagonal parts of image $f(x,y)$.

The inverse of 2-D DWT can be defined as:

$$f(x,y)=\frac{1}{MN}\sum_{m}\sum_{n}W_{\Phi}(j_0,m,n)\Phi_{j_0,m,n}(x,y)$$
$$+\frac{1}{MN}\sum_{i=H,V,D}\sum_{j=j_0}^{\infty}\sum_{m}\sum_{n}W^i_{\Psi}(j,m,n)\Psi^i_{j,m,n}(x,y) \tag{3}$$

3. Proposed simultaneous image fusion, encryption and compression technique

This section describes the proposed fusion, encryption and compression technique in detail.

3.1. Sparse representation

Let I_1 and I_2 are the two source images of size $M\times N$, for sparse representation, these images are transformed in frequency domain using DWT:

$$T_l=DWT(I_1) \tag{4}$$
$$U_l=DWT(I_2) \tag{5}$$

where, l represents the various subbands of source images and its values are $l=1,\ldots,4$ i.e. each of the transformed image T_l and U_l consist of four sub-bands namely, approximation (LL) and detail wavelet sub-bands $(LH,\ HL,\ HH)$. For example T_1,T_2,T_3 and T_4 represent the $LL_1, LH_1,\ HL_1,\ HH_1$ subbands of first source image respectively and U_1,U_2,U_3 and U_4 represent the $LL_2, LH_2,\ HL_2$, and HH_2 subbands of second source image respectively. The data amount of approximation sub-band is not sparse while the data amount of detail sub-band is sparse as most of the values in these sub-bands are close to zero, which can be seen from Fig. 1 and the schematic figure of proposed work is shown in Fig. 2

3.2. Fusion approach

After sparse representation of highly correlated data, the low and high frequency components are fused as follows: the difference between the approximation sub-bands of two source images is calculated as:

$$e(i,j)=LL_1(i,j)-LL_2(i,j),\qquad 1\leqslant i\leqslant M/2,\quad 1\leqslant j\leqslant N/2 \tag{6}$$

$$F_{LL}(i,j)=\begin{cases}LL_1(i,j)-e(i,j), & if(e(i,j))\leqslant 0\\ LL_2(i,j)+e(i,j), & otherwise\end{cases} \tag{7}$$

once the low frequency coefficients are fused, the next task is to fuse the detail wavelet coefficients: since detail wavelet coefficients contain the structural information, therefore, to retain the structural information maximum rule is applied to fuse the coefficients of these subbands.

$$F_{LH}(i,j)=\begin{cases}LH_2(i,j), & if(LH_1(i,j)\leqslant LH_2(i,j))\\ LH_1(i,j), & otherwise\end{cases} \tag{8}$$

$$F_{HL}(i,j)=\begin{cases}HL_2(i,j), & if(HL_1(i,j)\leqslant HL_2(i,j))\\ HL_1(i,j), & otherwise\end{cases} \tag{9}$$

$$F_{HH}(i,j)=\begin{cases}HH_2(i,j), & if(HH_1(i,j)\leqslant HH_2(i,j))\\ HH_1(i,j), & otherwise\end{cases} \tag{10}$$

3.3. Encryption and compression of fused information

After fusion of approximation and detail wavelet sub-bands: the fused approximation subband F_{LL} is encrypted using pseudo random numbers, as the approximation sub-band contain most of the useful information of the image, therefore first of all the coefficients of F_{LL} sub-band are quantized, the purpose is to decrease the range of wavelet coefficients.

$$Q_{LL}(i,j)=\left\lceil\frac{F_{LL}(i,j)-WC_{min}}{WC_{max}-WC_{min}}.q\right\rceil,\quad 1\leqslant i\leqslant M/2,\quad 1\leqslant j\leqslant N/2 \tag{11}$$

where, q represents a parameter, used to bound the values of F_{LL} subband in range $[0,q]$, here, $q=2^8-1$ and $\lceil.\rceil$ is the rounding operation, $WC(i,j)$ represents the wavelet coefficient of R_{LL} sub-band. The maximum and minimum values of coefficients in F_{LL} subband are represented by WC_{max} and WC_{min} respectively. The values of WC_{max} and WC_{min} are stream cipher encrypted and shared by the decoder. While, $Q_{LL}(i,j)$ represents the quantized wavelet coefficients. The quantization step which is used above, sets the values of R_{LL} sub-band in the range $[0,\ 255]$. Therefore, it is appropriate to choose an eight bit quantizer of resolution 8. After decreasing the range of F_{LL} sub-band, Q_{LL} subband is decomposed into four subimages as:

$$S_1(i,j)=Q_{LL}(2i,2j) \tag{12}$$

$$S_2(i,j)=Q_{LL}(2i,2j-1) \tag{13}$$

$$S_3(i,j)=Q_{LL}(2i-1,2j) \tag{14}$$

$$S_4(i,j)=Q_{LL}(2i-1,2j-1) \tag{15}$$

where, $1\leqslant i\leqslant M/4,\quad 1\leqslant j\leqslant N/4$. After downsampling, a single subimage S_1 is used to calculate the errors corresponding to other subimages as:

$$e_2(i,j)=S_2(i,j)-S_1(i,j) \tag{16}$$
$$e_3(i,j)=S_3(i,j)-S_1(i,j) \tag{17}$$

$$e_4(i,j)=S_4(i,j)-S_1(i,j), \tag{18}$$

Due to the high correlation among the neighboring pixels, most of the values in these sub-images are almost same, which result to small values in the errors, due to which fewer bits can be assigned on quantization and coding. For secure and efficient transmission of the fused low frequency coefficients, subimage S_1 is encrypted using pseudo random number sequences generated by pseudo random number generator (PRNG), equal to the number of elements in S_1, which lie within the range $[0,\ 255]$ and further addition modulo 256 is performed to form an encrypted image (Kumar et al., 2015).

$$E_1(i,j)=mod[S_1(i,j)+Ps(i,j),256],\quad 1\leqslant i\leqslant M/4,\quad 1\leqslant j\leqslant N/4 \tag{19}$$

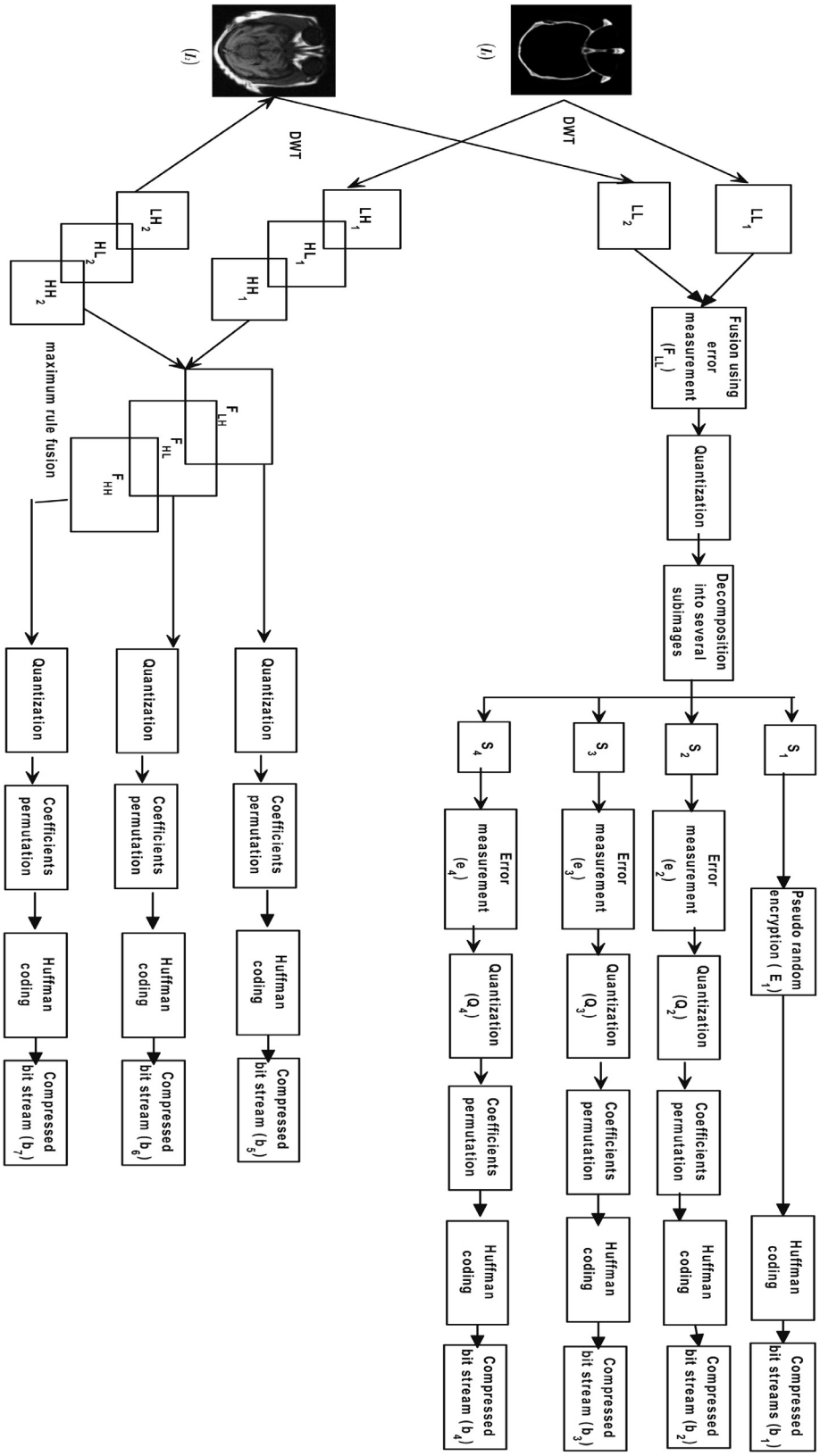

Fig. 2. Proposed scheme.

where, $Ps(i,j)$ shows the pseudo random number sequences generated by PRNG. Since sub-image S_1 consists most of the useful information of the image therefore, encrypted sub-image E_1 is compressed losslessly using huffman coding: as huffman coding is a lossless coding technique which can assign optimal bit codes. Let the compressed bit stream obtained be represented by b_1. After encrypting the sub-image S_1, the error corresponding to other sub-images are quantized as:

$$Q_2(i,j) = \lfloor (e_2(i,j)/p) \rfloor \tag{20}$$

$$Q_3(i,j) = \lfloor (e_3(i,j)/p) \rfloor \tag{21}$$

$$Q_4(i,j) = \lfloor \lfloor (e_4(i,j)/p) \rfloor \tag{22}$$

where, $1 \leqslant i \leqslant M/4, \quad 1 \leqslant j \leqslant N/4$ and p is a quantizing parameter shared by the decoder and the value of p is selected in such a way that we can achieve an acceptable image quality while saving large storage space, the quantitative value of p is discussed later in experimental result section. Due to the quantization, most of the values in the quantized errors Q_2, Q_3 and Q_4 become zero which results to more sparse data. For secure transmission of quantized errors, pseudo random permutation is used. Several permutation methods are reported in literature (Bourbarkis and Alexopoulos, 1992; Yen and Guo, 2000), but here in this work permutation method (Bourbarkis and Alexopoulos, 1992) is used for encryption. Further to assign optimal bits to each of the quantized errors, huffman coding is used, suppose the compressed bit streams are represented by b_2, b_3 and b_4 respectively.

After simultaneous compression and encryption of fused approximation subband, the detail wavelet coefficients are compressed and encrypted as: the data amount of detail wavelet subbands (F_{LH}, F_{HL} and F_{HH}) is reduced using the quantizing parameter p. As a result of quantization, most of these values are set to zero which led us to achieve better compression performance on coding. Before coding, the quantized coefficients are encrypted using pseudo random permutation. Due to the presence of large number of zeros in these sub-bands, the corresponding coefficients are compressed losslessly using huffman coding, which can assign the optimal codewords to the most frequent symbol. Let the compressed bit streams obtained after compression of these subbands be represented by b_5, b_6 and b_7 respectively.

The total amount of compressed data can be represented as:

$$B = \frac{(M \times N)}{4}(b_1 + b_2 + b_3 + b_4) + \frac{(M \times N)}{2}(b_5 + b_6 + b_7) \tag{23}$$

Further, the compression ratio (CR) i.e. a ratio between the amounts of original image data to the compressed data is expressed as:

$$CR = \frac{8 \times M \times N}{B} \tag{24}$$

3.4. Fused image reconstruction

The fused image can be reconstructed by using the proposed decompression and decryption approach. When having compressed bit streams ($b_1, b_2, b_3, b_4, b_5, b_6$ and b_7), each of these bit streams are decoded and decrypted. For decompression of low frequency components, the compressed bit stream b_1 is decoded using huffman decoding technique, suppose the decoded subimage is represented by E_1', which is followed by decryption process as:

$$S_1'(i,j) = mod[E_1'(i,j) - Ps(i,j), 256] \tag{25}$$

where, Ps shows the pseudo random numbers generated by using the same seed as used by encoder. The compressed bit streams b_2, b_3 and b_4 corresponding to the errors are decoded using huffman decoding technique, which result to quantized errors that are inverse permutated to get the decrypted quantized errors (say Q_2', Q_3' and Q_4'), these errors are de-quantized as Kumar and Vaish (2015):

$$E_2'(i,j) = \lfloor (Q_2'(i,j)p + (p-1)/2) \rfloor \tag{26}$$
$$E_3'(i,j) = \lfloor (Q_3'(i,j)p + (p-1)/2) \rfloor \tag{27}$$
$$E_4'(i,j) = \lfloor (Q_4'(i,j)p + (p-1)/2) \rfloor \tag{28}$$

where, $1 \leqslant i \leqslant M/4, \quad 1 \leqslant j \leqslant N/4$, once the errors are reconstructed, the low frequency components of other subimages can be recovered by simply adding these errors to the reconstructed subimage S_1' as:

$$S_2'(i,j) = S_1'(i,j) + E_2'(i,j) \tag{29}$$
$$S_3'(i,j) = S_1'(i,j) + E_3'(i,j) \tag{30}$$
$$S_4'(i,j) = S_1'(i,j) + E_4'(i,j) \tag{31}$$

now these subimages are upsampled to get the reconstructed low frequency components as:

$$Q_{LL}'(2i, 2j) = S_1'(i,j) \tag{32}$$

$$Q_{LL}'(2i, 2j-1) = S_2'(i,j) \tag{33}$$

$$Q_{LL}'(2i-1, 2j) = S_3'(i,j) \tag{34}$$

$$Q_{LL}'(2i-1, 2j-1) = S_4'(i,j) \tag{35}$$

Now, the values of Q_{LL}' is approximated with the help of decrypted WC_{max} and WC_{min} as:

$$F\prime_{LL} = \frac{Q_{LL}'(i,j)}{q}.(WC_{max} - WC_{min}) + WC_{min} \tag{36}$$

After obtaining the fused low frequency coefficients, the high frequency coefficients can be obtained by decoding the compressed bit streams b_5, b_6 and b_7. The obtained high frequency coefficients are inversely permuted to get the reconstructed subbands (say F_{LH}', F_{HL}' and F_{HH}').

The inverse of wavelet transform is then performed on fused low (F_{LL}') and high frequency coefficients (F_{LH}', F_{HL}' and F_{HH}') to obtain the reconstructed fused image (F').

4. Experimental results and discussion

The efficiency of proposed work is evaluated on various set of test images such as: mutlifocus, medical and visible-infrared images. In this section the detailed analysis on the security and compression performance of fused, encrypted and compressed image is presented.

4.1. Quality measurement of fused image

At the receiver side, the fused image can be reconstructed by simply decompressing and decrypting the compressed bit streams. The proposed work can reconstruct the fused image more efficiently with improved image quality while maintaining the security. Fig. 3 represents the fused images using various state of art methods along with the results of proposed work: Fig. 3(a) and 3 (b) show the Computed tomography (CT) and Magnetic Resonance (MR) source images, we have simulated the results for LP (Burt and Adelson, 1983), RP (Toet, 1989), DWT (Li et al., 1995), DTCWT (Lewis et al., 2007) and CVT (Nencini et al., 2007) methods and the corresponding results are shown in Fig. 3(c)–(g) respectively, while Fig. 3(h) shows the fused image using proposed SFEC rule. It can be analyzed from Fig. 3(h) that the proposed SFEC rule can reconstruct the fused image with improved image quality. The results corresponding to the proposed and compared methods for medical images are shown in Table 1. Various image quality measurement metrics such as: mutual information (MI), standard deviation (SD), correlation coefficient (CC), structural similarity index (SSIM) and peak signal to noise ratio (PSNR) are used to measure the quality of reconstructed fused images. It is evident from the quantitative results shown in Table 1 that the proposed SFEC technique is more effective than the existing one.

The proposed scheme is also applied on multi-focus image and the corresponding visual results are shown in Fig. 4. Fig. 4(a) and

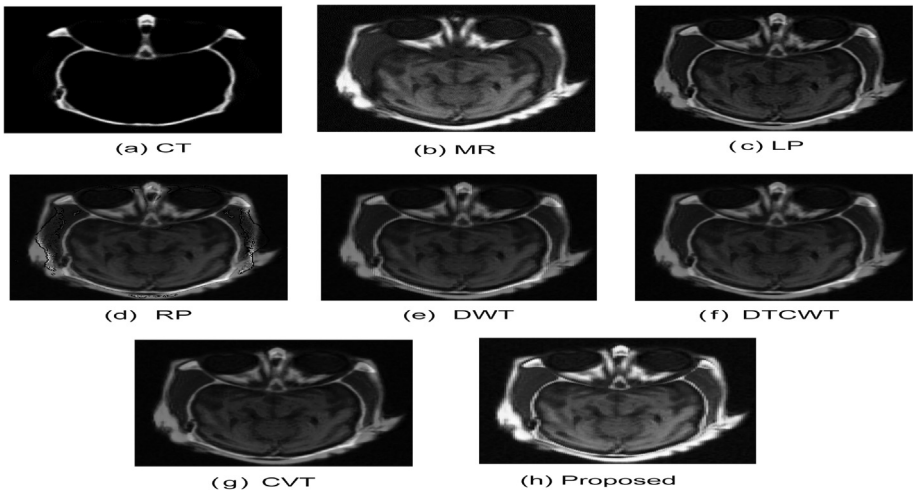

Fig. 3. Medical image fusion.

Table 1
Performance comparison of proposed work for Medical images with some existing works.

Fusion method	MI	SD	CC	SSIM	PSNR
LP (Burt and Adelson, 1983)	3.3657	35.9531	0.7133	0.4267	31.4400
RP (Toet, 1989)	4.5822	35.1517	0.6855	0.3931	31.7653
DWT (Li et al., 1995)	3.1765	34.0832	0.7064	0.4089	31.6553
DTCWT (Lewis et al., 2007)	4.1432	33.8704	0.7138	0.4199	31.5685
CVT (Nencini et al., 2007)	4.0868	33.7432	0.7134	0.4180	31.6058
Proposed	4.9995	58.5801	0.7620	0.4776	38.8047

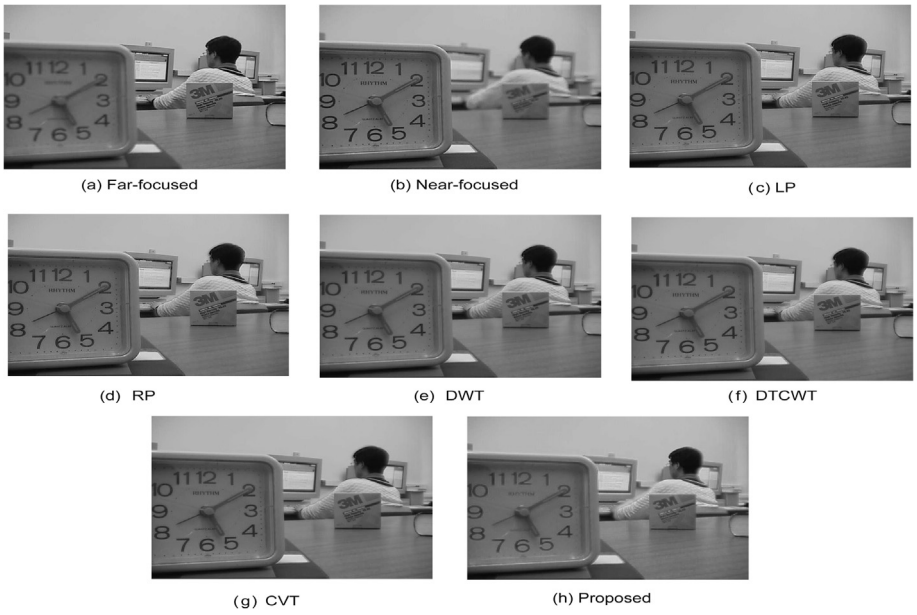

Fig. 4. Multi-focus images fusion.

(b) show the far and near focused images and the fused images using LP (Burt and Adelson, 1983), RP (Toet, 1989), DWT (Li et al., 1995), DTCWT (Lewis et al., 2007) and CVT (Nencini et al., 2007) fusion rules are shown in Fig. 4(c)–(g) respectively. The fused image using proposed SFEC rule is shown in Fig. 4(h). It can be observed from the visual results that the proposed scheme outperforms the several existing schemes. However, the visual quality of proposed work is also tested by measuring some mathematical terms and the corresponding results are shown in Table 2. For an example, when these source images are fused using LP (Burt and Adelson, 1983), RP (Toet, 1989), DWT (Li et al., 1995), DTCWT (Lewis et al., 2007) and CVT (Nencini et al., 2007) fusion rules, 36.7171 dB, 36.9352 dB, 36.4059 dB, 36.6062 dB and 36.5255 dB PSNR is obtained while when the same images are fused using proposed SFEC rule 42.1431 dB PSNR is obtained hence the proposed work can reconstruct the fused images with enhanced visual quality. Few more metrics are also used to evaluate the quality of fused image such as MI, SD, CC, SSIM, PSNR and the corresponding results

Table 2
Performance comparison of proposed work for multi-focus image with some existing works.

Fusion method	MI	SD	CC	SSIM	PSNR
LP (Burt and Adelson, 1983)	7.0752	46.1547	0.9844	0.9047	36.7171
RP (Toet, 1989)	7.0786	46.1053	0.9835	0.9033	36.9352
DWT (Li et al., 1995)	6.9175	45.5351	0.9856	0.9108	36.4059
DTCWT (Lewis et al., 2007)	7.0165	45.6051	0.9871	0.9184	36.6062
CVT (Nencini et al., 2007)	6.9474	45.5432	0.9871	0.9182	36.5255
Proposed	7.9572	44.7272	0.9969	0.9865	42.1431

are shown in Table 2, all the mathematical simulation shows that proposed work has obtained an improved image quality in case of all the metrics.

The quality of reconstructed fused image is also tested for visible and Infrared images. Fig. 5 demonstrates the result for these images using several existing and proposed schemes. The visible and infrared images are shown in Fig. 5(a) and (b) and the reconstructed fused images using existing methods are shown in Fig. 5 (c)–(g) respectively and the reconstructed fused image using proposed work is shown in Fig. 5(h). It can be noticed from the several results shown in Fig. 5 that the quality of proposed work is better than the other techniques. To test the efficiency of proposed work, some mathematical measures are also used and the corresponding results are shown in Table 3. Hence it can be observed from the Tables 1–3 that the proposed work is enhancing the visual quality for all type of source images.

4.2. Security analysis and compression performance evaluation

The proposed work is secure against various brute force attacks, as in case of natural image, the neighboring pixels have strong correlation and in this work the approximation (F_{LL}) and detail subbands (F_{LH}, F_{HL}, and F_{HH}) are encrypted using pseudo random number sequences and pseudo random permutation. Rather than directly masking the values of F_{LL} subband, it is decomposed into four subimages. A subimage is masked by using pseudo random number sequences while the errors are encrypted by using pseudo random permutation. The masking of most significant information makes the original image unrecognizable and also ensure the desired level of security because it is very well known that there is no probability polynomial time (PPT) algorithm is known to make a difference between pseudo random number sequences and random number sequence till now (Kumar et al., 2015; Kumar and Vaish, 2015). Hence, it is adequate to secure the image

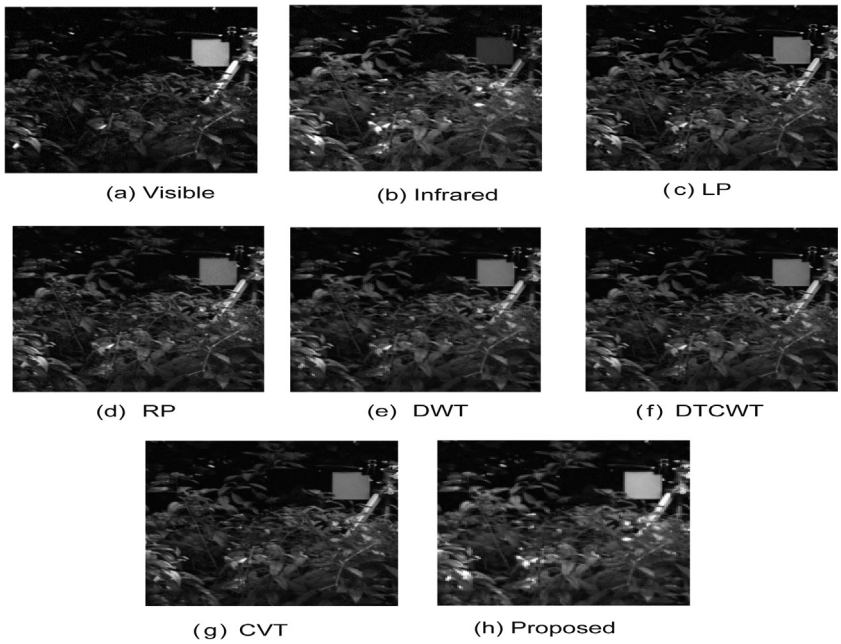

Fig. 5. Visible and Infrared images fusion.

Table 3
Performance comparison of proposed work for Visible-Infrared images with some existing works.

Fusion method	MI	SD	CC	SSIM	PSNR
LP (Burt and Adelson, 1983)	3.9439	33.4653	0.8709	0.8285	32.4216
RP (Toet, 1989)	3.8856	32.4710	0.8707	0.8240	33.0426
DWT (Li et al., 1995)	3.8940	31.5790	0.8717	0.8310	32.6801
DTCWT (Lewis et al., 2007)	4.1621	31.7324	0.8775	0.8458	32.6403
CVT (Nencini et al., 2007)	4.0716	31.6087	0.8775	0.8457	32.6333
Proposed	4.1183	41.7228	0.8966	0.8486	37.8928

information using pseudo random number sequences because it is harder for any PPT adversary to make a distinction between encrypted pixel sequence and a random number sequence. While the errors and detail wavelet coefficients consisting less significant information are pseudo randomly permutated, as the detail subbands contain the horizontal, vertical and diagonal details, which are quite sparse, hence it is sufficient to make a pseudo random permutation to hide the structural information. Since the values of detail wavelet subbands are not changed which infact maintain the empirical distribution of coefficients in the detail wavelet subbands, meanwhile these also help in improving the compression performance.

It is a point of consideration that the values of detail wavelet subbands and the errors corresponding to F_{LL} subband are not masked, instead of masking the values only pseudo random permutation is used. If there are T number of coefficients in the each of detail subband then there would be $T!$ ways to predict the position of each coefficient, here ! is the factorial operation. For an illustration, if the input image is of size 512×512, there are 256×256 i.e. 65,536 coefficients in each of the detail subbands and the number of elements in detail subbands is three times of that in approximation subband, an attempt of brute force search in these detail wavelet subbands requires $65,536!$ ways of permutation in each subband. For computational purpose the value of $65,536!$ can be assumed to infinity. Therefore, it is indeed hard for any attacker to implement brute force attack. Hence, the proposed technique has obtained a desired level of security and robustness against attacks.

The incorrectly decrypted fused image for medical image is shown in Fig. 6. Fig. 6(a) shows the reconstructed fused image using proposed scheme and its encrypted version is shown in Fig. 6(b), Fig. 6(b) is obtained when subimages encrypted by pseudo random number sequences and pseudo random permutation are incorrectly arranged. It can be observed from Fig.6(b) that the proposed work does not reveal any kind of original information. The encrypted image corresponding to reconstructed multi-focus fused image (Fig. 7(a)) is shown in Fig. 7(b). The reconstructed fused image corresponding to visible and infrared image is shown in Fig. 8(a) and its encrypted version is shown in Fig. 8 (b). In all the cases the incorrect parameter are chosen close to the original values. It can be observed from Figs. 6(b), 7(b) and 8 (b) that the proposed work has obtained a desired level of security

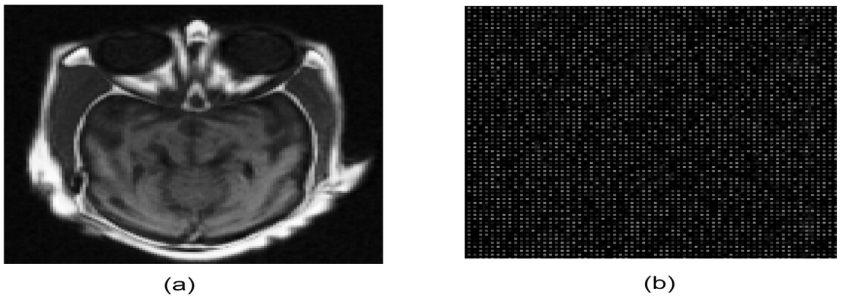

Fig. 6. (a) Correctly reconstructed medical fused image; (b) incorrectly reconstructed image.

Fig. 7. (a) Correctly reconstructed multi-focus image; (b) incorrectly reconstructed image.

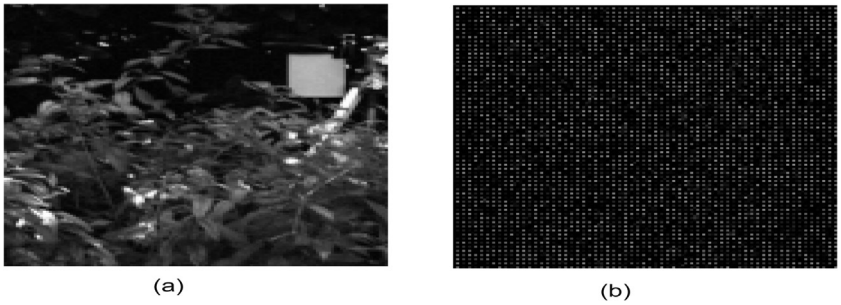

Fig. 8. (a) Correctly reconstructed Visible and Infrared fused image; (b) incorrectly reconstructed image.

Table 4
Compression performance measurement of proposed work.

Quantizing parameter (p)		8	12	16	20	24	28
Multifocus images	PSNR	42.3484	42.1829	42.1112	42.0525	42.0393	42.0191
	bpp	1.5733	1.5125	1.4861	1.4669	1.4632	1.4575
Medical images	PSNR	38.6925	38.6154	38.5762	38.5586	38.5485	38.5392
	bpp	1.7253	1.6425	1.5988	1.5727	1.5573	1.5349
Visible and infrared images	PSNR	37.8668	37.7269	37.6619	37.6235	37.6022	37.5875
	bpp	2.1962	1.9794	1.8740	1.8193	1.7861	1.7641

because untill the decoder does not have correct knowledge of encryption keys and way of arrangements, it would be hard to even guess a glimpse of original fused image.

The validity of proposed work is also evaluated by measuring compression performance. Several multi-source images are simultaneously fused, encrypted and compressed and a variation in the quality of reconstructed fused image with the reduced bit rate is evaluated. For the results shown in Tables 1–3, the quantizing parameter p is set to 14, the value is selected in order to achieve the good quality of reconstructed image while saving sufficient storage space. However, the relationship between the bit per pixel (bpp) and Peak Signal to Noise Ratio (PSNR) on various test images is shown in Table 4. It is evident from Table 4 that as the bpp decreases the quality of reconstructed fused image also decreases, although the degradation in the quality of reconstructed image is not perceptually visible to human eyes. Due to the proposed work, it is possible to reduce the size of fused images while maintaining the desired image quality. For an instance, when the multi-focus images are compressed using proposed scheme then 42.3484 dB PSNR is obtained for 1.5733 bpp, however, by increasing the qunatising parameter, better compression performance can be achieved without much more degradation in the visual quality of reconstructed images, which can be clearly observed from Table 4.

5. Conclusion

In this paper, a wavelet based simultaneous fusion, encryption and compression technique is proposed. The sparse representation of source images using DWT has helped in keeping salient features of source images in the reconstructed fused image. The low frequencies are fused using error based rule while the high frequency coefficients are fused using maximum fusion rule. The fused low and high frequency coefficients are simultaneously encrypted and compressed. The use of pseudo random number and pseudo random permutation in low and high frequency components respectively make the proposed scheme secure against any brute force attacks. The proposed scheme keeps the salient features of source images while enhancing the visual quality. The comparison of proposed work with several state of art works gives the evidence that the proposed work can reconstruct the fused images while maintaining the security of transmitting images. The compression performance of proposed work is also evaluated over the variation of quantizing parameter and it is found that the larger storage space can be saved by increasing the value of quantizing parameter. Hence the proposed work not only save the storage cost and security but also improves the visible quality the fused image.

References

Alfalou, A., Brosseau, C., 2009. Optical image compression and encryption methods. Adv. Opt. Photonics 1 (3), 589.

Alfalou, A., Loussert, A., Alkholidi, A., El Sawda, R., 2007. System for image compression and encryption by spectrum fusion in order to optimise image transmission, FGCN 2007. IEEE Proc. 2, 593–596.

Alfalou, A., Elbouz, M., Mansour, A., Keryer, G., 2010. New spectral image compression method based on an optimal phase coding and the RMS duration principle. J. Opt. 12.

Alfalou, A., Mansour, A., Elbouz, M., Brosseau, C., 2011. Optical Compression Scheme to Multiplex and Simultaneously Encode Images, Optical and Digital Image Processing Fundamentals and Applications. Wiley, NewYork. 463.

Alfalou, A., Brosseau, C., Abdallah, N., Jridi, M., 2011. Simultaneous fusion, compression, and encryption of multiple images. Opt. Exp. 24 (19).

Alfalou, A., Brosseau, C., Abdallah, N., Jridi, M., 2013. Assessing the performance of a method of simultaneous compression and encryption of multiple images and its resistance against various attacks. Opt. Exp. 21 (7).

Bhavana, V., Krishnappa, H.K., 2016. Fusion of MRI and PET images using DWT and adaptive histogram equalization. Communication and Signal Processing (ICCSP), 2016 International Conference on. IEEE.

Blum, R.S., Liu, Z., 2005. Multi-Sensor Image Fusion and Its Applications. CRC Press, Taylor and Francis Group.

Bourbarkis, N., Alexopoulos, C., 1992. Picture data encryption using SCAN patterns. Pattern Recognit. 25 (6), 567–581.

Burt, P., Adelson, E., 1983. The laplacian pyramid as a compact image code. IEEE Trans. Commun. 31 (4), 532–540.

Choi, Myungjin, Kim, Raeyoung, Nam, Myeongryong, Kim, Hongoh, 2005. Fusion of multispectral and panchromatic satellite images using the curvelet transform. IEEE Trans. Geosci. Remote Sens. Lett. 2 (2), 136–140.

Gonzalez, R.C., Woods, R.E., 2013. Digital Image Processing. Pearson Education, New Delhi, India.

Huang, R., Rhee, K.H., Uchida, S., 2012. A parallel image encryption method based on compressive sensing. Multimedia Tools Appl., 1–23

Jigneshkumar, M.P., Mehul, C.P., 2016. Medical image fusion based on MultiScaling (DRT) and MultiResolution (DWT) technique. In: International Conference on Communication and Signal Processing (ICCSP).

Kingsbury, N., 1999. Image processing with complex wavelets. In: Silverman, B., Vassilicos, J. (Eds.), Wavelets: The Key to Intermittent Information. Oxford University Press, pp. 165–185.

Kumar, M., Vaish, A., 2015. Prediction error based compression of encrypted images. International Conference on Computing and Communication Technology ACM, 228–232.

Kumar, Manoj, Vaish, Ankita, 2016. An Efficient Encryption-then-compression technique for Encrypted Images using SVD. Digital Signal Process. 60, 81–89.

Kumar, M., Vaish, A., 2015. An efficient compression of encrypted images using WDR coding. International Conference on Soft Computing for Problem Solving (SocPros-2015), 436 (4), 729–741.

Lewis, J., OCallaghan, R., Nikolov, S., Bull, D., Canagarajah, N., 2007. Pixel- and region based image fusion with complex wavelets. Inform. Fusion 8 (2), 119–130.

Li, H., Manjunath, B., Mitra, S., 1995. Multisensor image fusion using the wavelet transform. Graph. Models Image Process. 57 (3), 235–245.

Li, H., Manjunath, B., Mitra, S., 1995. Multisensor image fusion using the wavelet transform. Graph. Models Image Process 57 (3), 235–245.

Liu, Kun, Guo, Lei, Chen, Jingsong, 2011. Contourlet transform for image fusion using cycle spinning. J. Syst. Eng. Electron. 22 (2), 353–357.

Liu, X., Cao, Y., Lu, P., Lu, X., Li, Y., 2013. Optical image encryption technique based on compressed sensing and Arnold transformation. Optik 124 (24), 6590–6593.

Liu, Z., Yin, H., Fang, B., Chai, Y., 2014. A noval fusion scheme for visible and infrared images based on Compressive sensing. Opt. Commun.

Liu, X., Mei, W., Du, H., 2016. Simultaneous image compression,fusion and encryption algorithm based on compressive sensing and chaos. Opt. Commun. 366, 22–32.

Lu, P., Xu, Z., Lu, X., Liu, X., 2013. Digital image information encryption based on compressive sensing and double random-phase encoding technique. Optik 124 (16), 2514–2518.

Nencini, F., Garzelli, A., Baronti, S., Alparone, L., 2007. Remote sensing image fusion using the curvelet transform. Inform. Fusion 8 (2), 143–156.

Pajares, G., Cruz, J., 2004. A wavelet-based image fusion tutorial. Pattern Recognit. 37 (9), 1855–1872.

Toet, A., 1989. Image fusion by a ratio of low pass pyramid. Pattern Recognit. Lett. 9 (4), 245–253.

Wald, L., 1999. Some terms of reference in data fusion. IEEE Trans. Geosci. Remote Sens. 37 (3), 1190–1193.

Yen, J.C., Guo, J.I., 2000. Efficient Hierarchical chaotic image encryption algorithm and its VLSI realization. Proc. Inst. Elect. Eng. Vis. Image Signal Process. 147 (2), 167–175.

Zhou, N., Zhang, A., Zheng, F., Gong, L., 2014. Image compression-encryption hybrid algorithm based on key controlled measurement matrix in compressive sensing. Opt. Laser Technol. 62, 152–160.

Zhou, N., Zhang, A., Zheng, F., Gong, L., 2014. Novel image compression–encryption hybrid algorithm based on key-controlled measurement matrix in compressive sensing. Opt. Laser Technol. 62, 152–160.

Zhou, N., Zhang, A., Wu, J., Pei, D., Yang, Y., 2014. Novel hybrid image compression-encryption algorithm based on compressive sensing. Optik 125, 5075–5080.
Zhou, N., Li, H., Wang, D., Pan, S., Zhou, Z., 2015. Image compression and encryption scheme based on 2D compressive sensing and fractional Mellin transform. Opt. Commun. 343, 10–21.
Zhou, N., Li, H., Wang, D., Pan, S., Zhou, Z., 2015. Image compression and encryption scheme based on 2D compressive sensing and fractional Mellin transform. Opt. Commun. 343, 10–21.
Zhou, N., Pan, S., Cheng, S., Zhou, Z., 2016. Image compression–encryption scheme based on hyper-chaotic system and 2D compressive sensing. Opt. Laser Technol. 82, 121–133.
Zhu, H.G., Zhao, C., Zhang, X.D., 2013. A novel image encryption-compression scheme using hyper-chaos and chinese remainder theorem. Signal Process Image 28, 670–680.